Electronic Spectra of the MgC_4H and MgC_6H Radicals

Egor Chasovskikh, Evan B. Jochnowitz, and John P. Maier*

Department of Chemistry, University of Basel, Klingelbergstrasse 80, CH-4056, Basel, Switzerland

Received: May 6, 2008; Revised Manuscript Received: June 17, 2008

Electronic transitions of the linear MgC_4H and MgC_6H radicals have been observed in the gas phase using laser-induced fluorescence spectroscopy. The species were prepared in a supersonic expansion by ablation of a magnesium rod in the presence of acetylene, diacetylene, or methane gas. The transitions were recorded in the 445−446 nm region and assigned to the $A\ ^2\Pi-X\ ^2\Sigma^+$ systems (T_0 = 22 431.978(7) and 22 090.08(7) cm^{-1}) based on previously reported mass-selective resonance-enhanced ionization spectra and the rotational structure. A spectral fit in MgC_4H yields the rotational constants B'' = 0.04619(19) cm^{-1} for the $X\ ^2\Sigma^+$ state and B' = 0.04748(20) cm^{-1} for $A\ ^2\Pi$. Astrophysical implications are briefly addressed.

1. Introduction

Metal-containing molecules, such as MgCN, have been detected in the circumstellar envelopes of carbon-rich stars through radioastronomy.[1] Given the fact that Al and Mg are among the most common metallic elements found in the diffuse medium, one has to wonder whether carbon chains containing them might be responsible for the appearance of some of the diffuse interstellar bands, absorptions observed through diffuse clouds in the visible region.[2] In 1977 Douglas conjectured that carbon chains of size C_n, n = 5−10, might be responsible as carriers for some of bands;[3] however, thus far all gas-phase comparisons have proved negative.[4] Could metal-capped chains, which absorb in the proper visible region (400−800 nm) with sufficient oscillator strengths, be likely candidates?

Recently our group has reported the $A\ ^1\Pi-X\ ^1\Sigma^+$ spectrum of AlCCH in the gas phase.[5] Like its open-shelled counterpart, MgCCH, AlCCH clearly demonstrates a linear $\Pi-\Sigma$ transition. Previously, rotationally resolved electronic spectra of MgCCH radical were observed, yielding accurate rotational constants for the $A\ ^2\Pi-X\ ^2\Sigma^+$ system.[6,7] Other electronically observed metal-capped acetylides include the CaCCH and SrCCH radicals,[8] where detailed use of Stark spectroscopy led to determination of the dipole moment of the calcium-containing species.[9] As far as other metal monoacetylides are concerned, LiCCH,[10] NaCCH,[11] and KCCH[12] have all been shown to have linear $^1\Sigma^+$ ground states through rotational spectroscopy.

Only within the past year were the first gas-phase spectra of MgC_4H and MgC_6H obtained using a mass-selective resonant 2-color 2-photon ionization (R2C2PI) method with origin bands at 445.3 and 452.5 nm, respectively.[13] The systems were found to have significant oscillator strengths ($f \approx 0.1$) with the electronic excitation being localized on the Mg atom. Having the low-resolution R2C2PI spectra in hand, it was possible to investigate the $A\ ^2\Pi-X\ ^2\Sigma^+$ systems of MgC_4H and MgC_6H in more detail using the higher sensitivity afforded through laser-induced fluoresence. Note that only the origin band of the $A\ ^2\Pi-X\ ^2\Sigma^+$ MgC_4H system was investigated; as shown in previous mass-selective R2C2PI studies, exciting the Mg−C bond in the $A\ ^2\Pi$ state of MgC_4H results in a weak overlapping band with the origin system of MgCCH.[13]

* To whom correspondence should be addressed. Fax:+41-61-267-38-55. E-mail: j.p.maier@unibas.ch.

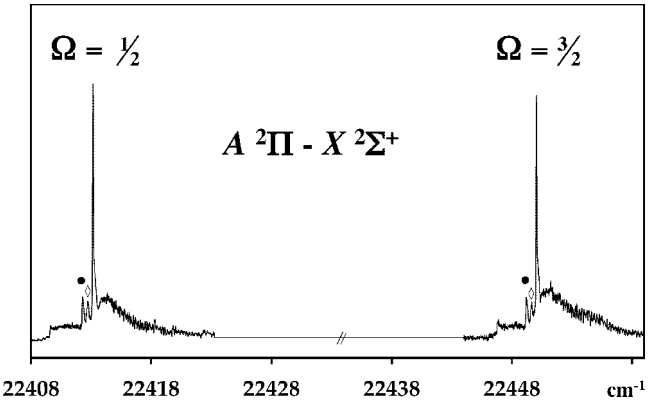

Figure 1. Observed Ω = 1/2 and 3/2 components of the origin band in the $A\ ^2\Pi-X\ ^2\Sigma^+$ electronic spectrum of MgC_4H measured using laser-induced fluorescence in a supersonic molecular beam. The main peaks are assigned to the most abundant isotopomer, $^{24}MgC_4H$, with $^{25}MgC_4H$ and $^{26}MgC_4H$ denoted by ◇ and ●, respectively.

2. Experimental Section

Jet-cooled MgC_nH was produced using laser vaporization (532 nm) of a pure magnesium rod in a flow of 5% acetylene, diacetylene, or methane in argon gas (10 bar) provided by a 0.3 mm orifice pulsed valve. The rod was rotated and translated so that a fresh surface was continuously exposed to the laser, which was fired to coincide with the gas flow over the target area. The vaporization plume flows through a channel (3 mm diameter by 5 mm long) before undergoing a free jet expansion. The resulting radicals are then probed through laser-induced fluorescence (LIF) using a Nd:YAG pumped dye laser (0.07 cm^{-1}) with a wavemeter used for frequency calibration (Burleigh WA4500). The fluorescence signal was collected by an *f*/1 lens and detected using a photomultiplier tube and a digital oscilloscope.

3. Results

3.1. MgC_4H. ***Identification of the Carrier.*** Figure 1 shows the excitation spectrum obtained in the 22408−22459 cm^{-1} region when ablating magnesium in the presence of methane. The LIF signal displayed a dependence on the presence of magnesium and hydrocarbon precursor. The general appearance of a PQR pattern with two spin−orbit components separated

10.1021/jp803969a CCC: $40.75
Published on Web 08/27/2008

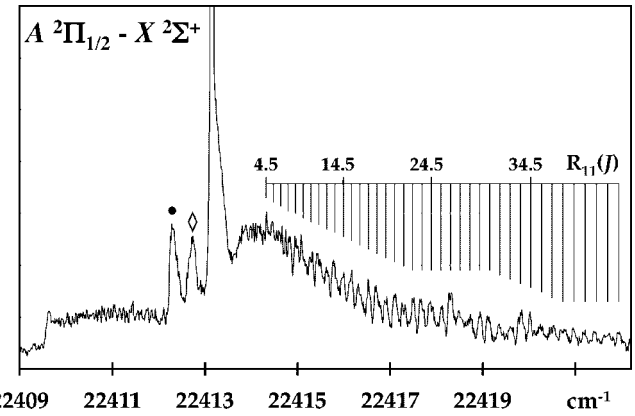

Figure 2. $\Omega = 1/2$ component in the origin band of the $A\ ^2\Pi - X\ ^2\Sigma^+$ electronic transition for MgC_4H. (◇ and ●) Less abundant species $^{25}MgC_4H$ and $^{26}MgC_4H$, respectively.

by nearly 37 cm^{-1} suggests a typical $^2\Pi - ^2\Sigma^+$ system. Previous ab initio calculations predict a linear $^2\Sigma^+$ ground-state structure with $C_{\infty v}$ symmetry.[13] The frequency positions determined from the low-resolution R2C2PI spectra of MgC_nH ($n = 2, 4, 6$) allowed an assignment of the observed bands with the symmetries of the transitions known on the basis of calculation; the bands depicted in Figure 1 clearly belong to MgC_4H. A band origin at 2.78 eV lies just below the vertical electronic excitation energy of 2.79 eV calculated for the $A\ ^2\Pi - X\ ^2\Sigma^+$ transition using TD-B3LYP methods combined with a cc-pVTZ basis set.[13] Furthermore, the rotational constants obtained are on the order of those expected from DFT calculations.

The nature of the spin−orbit band indicates the presence of a doubly degenerate excited electronic state. This doublet splitting of about 37 cm^{-1}, similar in magnitude to the spin−orbit splittings observed in other magnesium compounds, including MgH (35.3 cm^{-1}),[14] $MgCH_3$ (28.6 cm^{-1}),[15] MgNC (36.9 cm^{-1}),[16] and MgCCH (36.1 cm^{-1}),[7] further implies that the transition is metal centered and does not vary significantly with ligand size or composition.

Labeled in Figure 1 are two additional bandheads due to less abundant isotopic isomers of Mg, $^{25}MgC_4H$ (10%), and $^{26}MgC_4H$ (11%). While this observation allows an assignment of their origin location and excited-state spin−orbit splitting, their weak intensities and overlapping features precludes a proper rotational analysis for these minor constituents.

Rotational Structure. Modest resolution spectra were obtained with a Nd:YAG pumped dye laser (0.07 cm^{-1}). The trace in Figure 2 shows the $\Omega = 1/2$ spin−orbit component displayed in Figure 1. A similar profile was observed at 22450.46 cm^{-1} for $\Omega = 3/2$. The profile of the band fits that expected from a $^2\Pi - ^2\Sigma$ transition. With the spin−orbit constant $A \gg BJ$, the excited state of MgC_4H belongs to Hund's Case (a).

For MgC_4H, the strong bandheads in the $A\ ^2\Pi_{1/2} - X\ ^2\Sigma^+$ spin component are Q_{12} and P_{11}, while for the $A\ ^2\Pi_{3/2} - X\ ^2\Sigma^+$ spin component they are Q_{22} and P_{22}.[17] Fanning out to higher energy lie the R_{11}/R_{12} and R_{21}/R_{22} branches for the $\Omega = 1/2$ and 3/2 components, respectively, with the R_{11} and R_{21} lines being much higher in intensity and therefore suitable for rotational analysis. Also, in both the R_{11} and R_{21} branches line spacings are on the order of $3B$, allowing reasonable peak separation at the given resolution (0.07 cm^{-1}). In general, for such a $^2\Pi$ (case a)$-^2\Sigma^+$ (case b) transition one expects to observe rotational structure with line spacings of both $3B$ (R_{11}, R_{21}, P_{12}, and P_{22}) as well as B (R_{12}, R_{22}, P_{11}, and P_{21}) in the two spin−orbit components.

TABLE 1: Observed Rotational Lines (in cm^{-1}) of the Origin Band in the $A\ ^2\Pi - X\ ^2\Sigma^+$ Electronic Transition of $^{24}MgC_4H$[a]

	$A\ ^2\Pi_{1/2} - X\ ^2\Sigma^+$		$A\ ^2\Pi_{3/2} - X\ ^2\Sigma^+$	
	R_{11} branch		R_{21} branch	
J	$\tilde{\nu}_{obs}$	$\tilde{\nu}_{obs} - \tilde{\nu}_{calcd}$	$\tilde{\nu}_{obs}$	$\tilde{\nu}_{obs} - \tilde{\nu}_{calcd}$
4.5	22414.332	0.006		
5.5	22414.489	0.007		
6.5	22414.646	0.007		
7.5	22414.816	0.017	22451.676	−0.002
8.5	22414.956	−0.005	22451.847	0.005
9.5	22415.116	−0.010	22452.005	−0.004
10.5	22415.287	−0.007	22452.169	−0.010
11.5	22415.482	0.020	22452.345	−0.006
12.5	22415.629	−0.005	22452.528	0.002
13.5	22415.804	−0.004	22452.701	−0.004
14.5	22415.991	0.006	22452.886	0.001
15.5	22416.170	0.006	22453.071	0.003
16.5	22416.358	0.011	22453.248	−0.007
17.5	22416.531	−0.001	22453.435	−0.009
18.5	22416.715	−0.002	22453.620	−0.015
19.5	22416.901	−0.006	22453.834	0.005
20.5	22417.097	−0.002	22454.032	0.006
21.5	22417.301	0.008	22454.230	0.003
22.5	22417.486	−0.003	22454.426	−0.003
23.5	22417.669	−0.020	22454.628	−0.007
24.5	22417.899	0.009	22454.844	0.002
25.5	22418.107	0.012	22455.067	0.015
26.5	22418.301	−0.007	22455.268	0.003
27.5	22418.498	−0.012	22455.470	−0.012
28.5	22418.733	0.011	22455.709	0.008
29.5	22418.943	0.007	22455.942	0.020
30.5	22419.121	−0.031	22456.136	−0.011
31.5	22419.356	−0.015	22456.360	−0.013
32.5	22419.611	0.018	22456.606	0.003
33.5	22419.838	0.021	22456.834	−0.001
34.5	22420.022	−0.021	22457.068	−0.002
35.5	22420.270	−0.002	22457.298	−0.011
36.5	22420.538	0.034	22457.554	0.006
37.5	22420.752	0.014	22457.779	−0.013
38.5	22420.957	−0.017	22458.040	0.002
39.5	22421.201	−0.012	22458.291	0.004
40.5	22421.417	−0.037	22458.549	0.011
41.5	22421.715	0.018	22458.799	0.007
42.5	22421.940	−0.004	22459.046	−0.003
43.5	22422.216	0.024	22459.306	−0.003
44.5	22422.428	−0.016	22459.588	0.017
45.5	22422.694	−0.003	22459.845	0.009
46.5	22422.952	−0.001	22460.106	0.003
47.5	22423.198	−0.014	22460.374	0.001

[a] The uncertainty of the $\tilde{\nu}_{obs}$ values given is judged to be ± 0.007 cm^{-1}.

A rotational fit was performed for a $^2\Pi - ^2\Sigma^+$ transition in a linear molecule using the PGOPHER program.[18] The calculated spectrum was obtained by first varying the rotational parameters B'' and B', the excited state's spin−orbit coupling constant, as well as the line width, temperature, and origin assignment. At this resolution, lines belonging to the R_{11} and R_{21} branches could be singled out due to their greater peak separation ($\sim 3B$). Rotational line assignments were made by comparing the observed spectral lines with those calculated. A spectral least-squares fit using 85 R-branch lines could be performed, allowing the determination of six varied spectroscopic parameters at a temperature of 50 K and a line width fixed at 0.07 cm^{-1} (Tables 1 and 2). Variations in line intensities of the experimental spectra are mainly due to instability in the ablation source. Higher

TABLE 2: Constants Determined from the Analysis of the Electronic Spectrum of $^{24}MgC_4H$[a]

parameter	$X\ ^2\Sigma^+$	$A\ ^2\Pi$
T_0/cm^{-1}		22431.978(7)
B/cm^{-1}	0.04619(19)	0.04748(20)
A/cm^{-1}		36.964(3)

[a] Values in parentheses denote the 2σ standard deviation from the fit.

TABLE 3: Origin Band Wavenumbers and Spin−Orbit Constants for the $A\ ^2\Pi-X\ ^2\Sigma^+$ Transition in the MgC_4H Isotopomers[a]

	$^{24}MgC_4H$	$^{25}MgC_4H$	$^{26}MgC_4H$
T_0/cm^{-1}	22431.978(7)	22431.53(7)	22431.11(7)
A/cm^{-1}	36.964(3)	36.97(7)	36.99(7)

[a] Constants obtained for $^{25}MgC_4H$ and $^{26}MgC_4H$ from measurement of the band head positions and not from a rotational analysis.

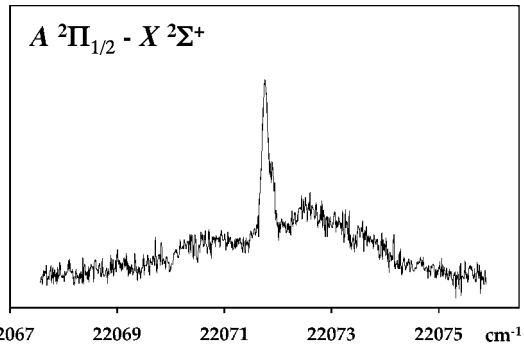

Figure 3. $\Omega = 1/2$ component in the origin band of the $A\ ^2\Pi-X\ ^2\Sigma^+$ electronic transition for MgC_6H measured using laser-induced fluorescence in a supersonic molecular beam, featuring the prominent Q_{12}/P_{11} bandhead.

resolution experiments will be required to identify spectroscopic terms with a larger degree of accuracy using additional weaker R_{12}/R_{22} lines which could not be distinguished currently due to the spectral density that results from their smaller spacings ($\sim B$). Likewise, the shape of the bandhead and overlapping isotopic species made individual assignment of any P- and Q-branch lines impossible.

The two isotopic isomers ($^{25}MgC_4H$ and $^{26}MgC_4H$) located to the red of the major abundant species ($^{24}MgC_4H$) clearly contribute to the band profile observed in the experimental spectrum in Figure 1. For these less abundant species their band origin T_0 and spin−orbit constant A were varied until a reasonable visual agreement was achieved with the experiment (Table 3). A least-squares fit was not attempted due to the weakness of their overlapping features. While the presence of these isotopomers made the assignment of any P-branch lines difficult, they did not, however, interfere with lines from the R_{11}/R_{21} branches of the major $^{24}MgC_4H$ species and thus do not lead to any discrepancies concerning its rotational fit. The ground-state rotational constant B'' obtained, 0.04619(19) cm^{-1}, agrees reasonably with the literature calculated values of 0.04612 and 0.04508 cm^{-1} for the B3LYP and RCCSD(T) methods, respectively.[13]

Time profiles of the fluorescence decay were measured by tuning the laser frequency to the bandhead of each spin−orbit component in the $A\ ^2\Pi-X\ ^2\Sigma^+$ transition of MgC_4H, yielding fluoresence lifetimes on the order of 35 ns.

3.2. MgC_6H. Figure 3 shows the $A\ ^2\Pi_{1/2}-X\ ^2\Sigma^+$ electronic transition for MgC_6H, located at 22071.94 cm^{-1}. The less intense $A\ ^2\Pi_{3/2}-X\ ^2\Sigma^+$ component was located at 22108.22 cm^{-1}. Clearly evident is how the general shape of the $\Omega = 1/2$ band resembles that of MgC_4H, shown in Figure 2, with a well-defined Q_{12}/P_{11} branch head. As before, tests involving the presence of magnesium and hydrocarbon precursor, 37 cm^{-1} spin−orbit splitting, general appearance of a PQR pattern, and previous knowledge of the spectral region to interrogate in addition to mass-selective R2C2PI spectra[13] all confirmed the assignment of the spectral carrier.

The experimental band origin, $T_0 = 22090.08$ cm^{-1} (2.74 eV), lies a bit above the vertical excitation energy of 2.65 eV calculated for the $A\ ^2\Pi-X\ ^2\Sigma^+$ transition using TD-B3LYP methods. Calculations predict a rotational constant of about 0.019 cm^{-1}, making the present experimental resolution of 0.07 cm^{-1} insufficient to resolve the B or even the $3B$ spacings expected for individual lines. As far as locating the two isotopic isomers ($^{25}MgC_6H$ and $^{26}MgC_6H$), we believe that their weak bandheads must be obscured by the presence of the $^{24}MgC_6H$ species with spectral congestion further prohibiting any clear assignment.

While individual rotational lines could not be assigned due to both the resolution used and the band's weak intensity, visually varying T_0 and A in the $A\ ^2\Pi$ state led to an origin assignment of 22090.08(7) cm^{-1} and a spin−orbit coupling constant of 36.28(7) cm^{-1}. Decay profiles of the MgC_6H band indicate a fluorescence lifetime just shorter than MgC_4H, at about 28 ns.

TABLE 4: Origin Band Positions and Calculated Vertical Excitation Energies (in eV) for the $A\ ^2\Pi-X\ ^2\Sigma^+$ Transition in the MgC_nH Series

	experiment	B3LYP[a]	RCCSD(T)[a]
MgC_2H	2.83[b]	2.92	2.87
MgC_4H	2.78	2.79	2.84
MgC_6H	2.74[c]	2.65	2.81

[a] Reference 13. [b] Reference 7. [c] From measurement of the band head positions and not from a rotational analysis.

4. Discussion

The experimental origin band positions for the MgC_nH, $n = 2, 4, 6$, are given in Table 4 along with the previously calculated vertical transition energies. Although a simple TD-DFT method assumes the same geometry in the ground and excited states, decent agreement (~0.1 eV) is found with the experimental result when compared with the entire series. Thus, the TD-DFT predictions support the spectral assignments. Moreover, the assignments are consistent with previous mass-selective R2C2PI spectra and therefore resolve any ambiguity.

Earlier, potential-energy curves were calculated for the $X\ ^2\Sigma^+$ ground and $A\ ^2\Pi$ states of MgC_4H as a function of the Mg−C coordinate using the RCCSD(T)/cc-pVTZ level of theory.[13] While the Mg−C bond length is shorter in the excited state, it was argued that the bonding energy in the ground state is actually stronger than that in the $A\ ^2\Pi$ state (dissociation energies of 327.6 versus 69.0 kJ mol^{-1}). Weak bonding in the excited state was partially rationalized by an avoided crossing with the $B\ ^2\Pi$ state. The shorter bond length can be explained using molecular orbital arguments, where excitation from an anti-bonding semioccupied MO to the LUMO leads to bond length contraction, thus accounting for the experimentally observed increase in rotational constant upon excitation.[13,19]

An important aspect of the magnesium-capped chains is their astrophysical significance. As stated earlier, Mg-containing

species have already been detected in carbon-rich stars. Previous calculations have investigated the oscillator strengths of these transitions, which are of interest for astrophysical observation. While the dipole moment increases monotonically with the size of the chain, the oscillator strength of the specific $A\ ^2\Pi-X\ ^2\Sigma^+$ transition in MgC_nH is calculated to decrease.[13] This behavior differs from that of the polyyne $HC_{2n+1}H$ chains, which has been attributed to the fact that there the f values arise from a delocalized π-electron excitation.[20] In the case of the magnesium-capped chains, the transition arises from promotion of a σ-electron localized on the metal atom. Thus, as the chain becomes larger with increasing n, delocalization on the chain acts to remove oscillator strength when the σ electron is excited.

The possibility of MgC_4H being a reasonably good candidate for the unassigned B1395 lines detected in the envelope of carbon-rich star IRC+10216 has been previously addressed.[21] In particular, the features observed are said to originate from an unidentified linear $^2\Sigma$ species with $B_0 = 1.3946$ GHz. While initial considerations point to MgCCCN as the carrier, discussions suggest that MgC_4H also remains viable; both species have identical ground-state $^2\Sigma$ symmetries and similar rotational constants (B_0(corrected) = 1.3925 and 1.3972 GHz at the B3LYP/aug-DZ level of theory for MgCCCN and MgC_4H, respectively.) In the same star Mg- and Al-containing species such as MgNC,[22] MgCN,[1] AlNC,[23] AlCl,[24] and AlF[25] have all been previously observed. It has also been postulated that species such as C_2H, C_4H, and C_6H could be formed in the star's outer shell as the result of photodissociation mechanisms involving CO, C_2H_2, and HCN.[26] However, the lack of detection of the smaller MgCCH radical in IRC+101216 seems to imply even lower abundances for MgC_4H.[21]

Another important consequence of the Mg-terminated chains is the fact that their $A\ ^2\Pi-X\ ^2\Sigma^+$ electronic transitions occur in the diffuse interstellar band 400−700 nm window. A comparison with the tabulations of the latter absorptions resulted in no corresponding matches.[27] Of note is the fact that the $A\ ^2\Pi-X\ ^2\Sigma^+$ excitation in MgC_4H is not the most intense transition. Calculations of the vertical excitation energies using TD-DFT have shown that there are indeed two higher lying and as of yet undetected excitations: $A\ ^2\Pi-X\ ^2\Sigma^+$ (2.79 eV, $f = 0.09$), $B\ ^2\Pi-X\ ^2\Sigma^+$ (3.05 eV, $f = 0.02$), and $C\ ^2\Sigma^+-X\ ^2\Sigma^+$ (4.49 eV, $f = 0.29$).[13]

5. Conclusions

The rotationally resolved laser excitation spectrum of the origin band for the $A\ ^2\Pi-X\ ^2\Sigma^+$ band of MgC_4H has been observed and analyzed. A spectral fit yields rotational constants for the ground and first excited states, allowing for further investigations into this important class of metal-capped carbon chains, which may aid the search for the millimeter-wave spectrum of MgC_4H in the laboratory. Weak electronic absorption for the larger MgC_6H radical has been observed. Poor production and a smaller oscillator strength as well as line spacings which are unresolvable at the current resolution prohibited a proper rotational analysis; however, the origin band location and spin−orbit splitting could be estimated. These data provide the means of identifying the MgC_nH, $n = 4$ and 6, species in various environments by electronic spectroscopy.

Acknowledgment. This work was supported by the Swiss National Science Foundation (project no. 200020115864/1) and the European Office of Aerospace Research and Development (Grant FA8655-07-1-30310) and is part of the European Union project "Molecular Universe" (MRTN-CT-2004-512303).

References and Notes

(1) Ziurys, L. M.; Apponi, A. J.; Guelin, M.; Cernicharo, J. *Astrophys. J.* **1995**, *445*, L47.
(2) Herbig, G. H. *Annu. Rev. Astron. Astrophys.* **1995**, *33*, 19.
(3) Douglas, A. E. *Nature* **1977**, *269*, 130.
(4) Maier, J. P.; Walker, G. A. H.; Bohlender, D. A. *Astrophys. J.* **2004**, *602*, 286.
(5) Apetrei, C.; Ding, H.; Maier, J. P. *Phys. Chem. Chem. Phys.* **2007**, *9*, 3897.
(6) Corlett, G. K.; Little, A. M.; Ellis, A. M. *Chem. Phys. Lett.* **1996**, *249*, 53.
(7) Tokaryk, D. W.; Adam, A. G.; Hopkins, W. S. *J. Mol. Spectrosc.* **2005**, *203*, 54.
(8) Dick, M. J.; Sheridan, P. M.; Wang, J. G.; Bernath, P. F. *J. Mol. Spectrosc.* **2005**, *233*, 197–202.
(9) Marr, A. J.; Perry, J.; Steimle, T. C. *J. Chem. Phys.* **1995**, *103*, 3861.
(10) Apponi, A. J.; Brewster, M. A.; Ziurys, L. M. *Chem. Phys. Lett.* **1998**, *298*, 161.
(11) Grotjahn, D. B.; Apponi, A. J.; Brewester, M. A.; Xin, J.; Ziurys, L. M. *Angew. Chem., Int. Ed.* **1998**, *37*, 2678.
(12) Xin, J.; Ziurys, L. M. *Astrophys. J.* **1998**, *501*, L151.
(13) Ding, H.; Apetrei, C.; Chacaga, L.; Maier, J. P. *Astrophys. J.* **2008**, *627*, 348.
(14) Huber, K. P.; Herzberg, G. *Constants of diatomic molecules*; Van Nostrand-Rheinhold: Princeton, 1979.
(15) Rubino, R.; Williamson, J. M.; Miller, T. A. *J. Chem. Phys.* **1995**, *103*, 5964.
(16) Wright, R. R.; Miller, T. A. *J. Mol. Spectrosc.* **1999**, *194*, 219.
(17) Herzberg, G. *Spectra of Diatomic Molecules*; Van Nostrand-Rheinhold: New York, 2nd ed., 1950.
(18) Western, C. M. *PGOPHER, a Program for Simulating Rotational Structure*; University of Bristol, 2007; http://pgopher.chm.bris.ac.uk.
(19) Woon, D. E. *Chem. Phys. Lett.* **1997**, *274*, 299.
(20) Ding, H.; Schmidt, T. W.; Pino, T.; Boguslavskiy, A. E.; Güthe, F.; Maier, J. P. *J. Chem. Phys.* **2003**, *119*, 814.
(21) Petrie, S.; Kagi, E.; Kawaguchi, K. *Mon. Not. R. Astron. Soc.* **2003**, *343*, 209.
(22) Kawaguchi, K.; Kagi, E.; Hirano, T.; Takano, S.; Saito, S. *Astrophys. J.* **1993**, *406*, L39.
(23) Ziurys, L. M.; Savage, C.; Highberger, J. L.; Apponi, A. J.; Guelin, M.; Cernicharo, J. *Astrophys. J.* **2002**, *564*, L45.
(24) Cernicharo, J.; Guelin, M. *Astron. Astrophys.* **1987**, *183*, L10.
(25) Ziurys, L. M.; Apponi, A. J.; Philips, T. G. *Astrophys. J.* **1994**, *433*, 729.
(26) Cherchneff, I.; Glassgold, A. E. *Astrophys. J.* **1993**, *419*, L41.
(27) Jenniskens, P.; Desert, F. X. *Astron. Astrophys.* **1994**, *106*, 39.

JP803969A